Carcinogenesis vol.31 no.10 pp.1726–1733, 2010
doi:10.1093/carcin/bgq160
Advance Access publication July 30, 2010

The miR-217 microRNA functions as a potential tumor suppressor in pancreatic ductal adenocarcinoma by targeting KRAS

Wu-Gan Zhao, Shuang-Ni Yu, Zhao-Hui Lu, Yi-Hui Ma, Yu-Mei Gu and Jie Chen*

[1]Department of Pathology, Peking Union Medical College Hospital, Chinese Academy of Medical Sciences and Peking Union Medical College, Tsinghua University, 1 Shuai Fu Yuan Hu Tong, Beijing 100730, People's Republic of China

*To whom correspondence should be addressed. Tel: +86 10 6529 5490; Fax. +86 10 6529 5490;
Email: xhblk@163.com

Aberrantly expressed microRNA (miRNA) is frequently associated with a variety of cancers, including pancreatic ductal adenocarcinoma (PDAC). In this study, we investigated the expression and possible role of miR-217 in PDAC. Data obtained by locked nucleic acid *in situ* hybridization and real-time quantitative polymerase chain reaction showed that miR-217 was downregulated in 76.2% (16/21) of PDAC tissues and in all tested PDAC cell lines when compared with the corresponding normal pancreatic tissue. Overexpression of miR-217 in PDAC cells inhibited tumor cell growth and anchorage-independent colony formation and miR-217 decreased tumor cell growth in nude mouse xenografts *in vivo*. Using *in silico* predictions, KRAS was defined as a potential direct target of miR-217. Data from the dual-luciferase reporter gene assay showed that KRAS was a direct target of miR-217. Upregulation of miR-217 could decrease KRAS protein levels and reduce the constitutive phosphorylation of downstream AKT. Downregulation of miR-217 expression in PDAC cells could increase cell anchorage-independent colony formation and KRAS protein levels. Furthermore, miR-217 expression was observed to be negatively correlated with KRAS protein expression in PDAC cell lines. We conclude that the frequently downregulated miR-217 can regulate KRAS and function as a tumor suppressor in PDAC. Therefore, miR-217 may serve as a useful therapeutic agent for miRNA-based PDAC therapy.

Introduction

Pancreatic ductal adenocarcinoma (PDAC) is one of the most devastating human malignancies, with an overall 5 year survival rate <5% and a median survival time of 6 months. Moreover, the almost identical annual incidence and mortality rates make it the fourth leading cause of cancer-related death worldwide (1–4). The major biological hallmarks of PDAC are its early and aggressive local invasion, metastasis and resistance to chemotherapy and radiotherapy. These traits probably contribute to the observation that the vast majority of patients presenting with advanced disease cannot be cured. The molecular basis for these characteristics of pancreatic cancer is not completely understood.

MicroRNAs (miRNAs) are endogenous non-coding RNAs consisting of 19–24 nucleotides that play important roles in the negative regulation of gene expression by base pairing to complementary sites in the target messenger RNA (mRNA) 3′-untranslated region (UTR), thus causing a block in the translation or the degradation of the target mRNAs (5). Mounting evidence indicates that miRNAs are aberrantly expressed in different types of tumors and play key roles in tumorigenesis (6–8). Recently, a number of miRNAs called oncomirs that appear to function as oncogenes or tumor suppressor have been identified (9). The downregulation of a subset of miRNAs implies a tumor suppressor function. For example, as a potential growth suppressor, downregulated let-7 in human colon cancer cells can target RAS (10). Deleted or downregulated miR-15 and miR-16 in chronic lymphocytic leukemia suppress Bcl2 (11). MiR-143 and miR-145 have been shown to function in tumor suppression because the overexpression of both miR-143 and miR-145 in human gastric cancer cells with low endogenous expression of these miRNAs significantly inhibits cell growth (12). The current miRNA registry database (release 13.0, March 2009) consists of 706 human miRNA genes (13). However, most of these genes, which are aberrantly expressed in cancers, need to be functionally defined.

A comparison of the results obtained for the miRNA expression profiles of PDAC with those for normal pancreas showed that the presence of miR-216 and miR-217 and the lack of miR-133a expression were characteristic of pancreatic tissues. Twenty-six miRNAs were aberrantly expressed in PDAC, of which only miR-217 and miR-196a were found to be differentially expressed in normal pancreas, chronic pancreatitis and cancerous tissues (14). Regarding the function of miR-217, previous work has demonstrated that it can target oncogenes or tumor suppressor genes in different cell type-specific backgrounds. For example, miR-217 can target silent information regulator 1 (SirT1), which modulates endothelial cell senescence (15) and has been shown to function as an oncogene (16–18). In addition, miR-217 can also target the tumor suppressor gene *PTEN* in kidney disorders (19). However, no specific studies have been conducted to investigate the role of miR-217 in PDAC.

In the present study, we investigated the expression and role of miR-217 in human PDAC. First, we evaluated the expression of miR-217 in PDAC tissues, paired adjacent normal pancreatic tissues and PDAC cell lines. Second, to investigate the functional roles of miR-217 in PDAC, we examined the tumor cell growth, anchorage-independent colony formation and xenografts tumor growth following upregulation or downregulation of miR-217. Finally, we determined the target gene of miR-217 using *in silico* prediction and the luciferase reporter assay.

Abbreviations: miRNA, microRNA; mRNA, messenger RNA; PCR, polymerase chain reaction; PDAC, pancreatic ductal adenocarcinoma; qPCR, quantitative polymerase chain reaction; RTV, relative tumor volume; UTR, untranslated region; WT, wild-type.

Materials and methods

Cell lines and human tissue samples

The human PDAC cell lines, including PANC-1, MIAPaCa-2, AsPC-1 and BxPC-3 cells, were purchased from the American Type Culture Collection (Rockville, MD); P1, P3 and P7 were constructed in our laboratory (20). All cells except MIAPaCa-2 were cultured in RPMI-1640 medium (Invitrogen, Carlsbad, CA) supplemented with 10% fetal calf serum (Gemini Bio-Products, Woodland, CA) at 37°C in a humidified atmosphere containing 5% CO_2. MIAPaCa-2 cells were cultured in Dulbecco's Modified Eagle's Medium. Tissues were obtained from patients undergoing PDAC surgery, collected immediately, snap frozen in liquid nitrogen and stored at −80°C until RNA extraction. After approval from the institutional review board, 21 formalin-fixed paraffin-embedded PDAC specimens and 21 paired adjacent normal pancreas samples were obtained from the Department of Pathology's archival files at the Peking Union Medical College Hospital, China. All patients provided written informed consent for the use of their tissues. This project was approved by the Peking Union Medical College Hospital Clinical Research Ethics Committee, China.

In situ hybridization

Locked nucleic acid probes of the complement to human mature miR-217 (5′-TACTGCATCAGGAACTGATTGGAT-3′), the scrambled negative control and the U6 positive control, which were digoxigenin-labeled at the 3′ position and purchased from Exiqon (Vedbaek, Denmark). Detection of the RNAs by *in situ* hybridization utilizing the oligonucleotide probes was performed according to the manufacturer's instructions. Briefly, human tissues were deparaffinized, treated with proteinase K (5 min in 2 μg/ml protease K), washed in sterile diethypyrocarbonate-treated phosphate-buffered saline and subsequently

© The Author 2010. Published by Oxford University Press. All rights reserved. For Permissions, please email: journals.permissions@oxfordjournals.org

Downloaded from https://academic.oup.com/carcin/article/31/10/1726/2477236 by guest on 24 April 2024

fixed with 4% paraformaldehyde. After prehybridization, hybridization was performed at 51°C overnight, followed by a stringency wash in 2× standard saline citrate and 50% formamide and 3 × 30 min washes at 51°C in 2× standard saline citrate. After blocking (2% sheep serum and 2 mg/ml bovine serum albumin in phosphate buffered saline with Tween-20) at room temperature, the probe–target complex was visualized utilizing a digoxigenin antibody conjugated to alkaline phosphatase, which acts on the chromogen nitroblue tetrazolium/5-bromo-4-chloro-3-indolyl phosphate. The slides were then independently scored by at least two pathologists as negative (−), weak or focally positive (1+) or strongly positive (2+) (21).

RNA isolation and real-time quantitative polymerase chain reaction analysis

Total RNA was extracted using TRIzol reagent (Invitrogen). For the detection of *KRAS* mRNA, first strand complementary DNA was synthesized from 1 μg of total RNA in the presence of oligo-dT (12–18) primer (Takara, Otsu, Shiga, Japan) and MMLV reverse transcriptase according to the manufacturer's instructions (Promega Corporation, Madison, WI). Human glyceraldehyde 3-phosphate dehydrogenase RNA was amplified in parallel as an internal control. For miR-217 detection, 1 μg of total RNA was used in the reverse transcriptase reaction with the miR-217-specific hairpin reverse primer (217-RT) (22). The primers used to amplify mature miR-217 were designed according to Chen *et al.* (22). Human *U6* RNA was amplified as the internal control. Real-time quantitative polymerase chain reaction (qPCR) was performed with SYBR Green PCR Master Mix using an IQ5 Real-Time PCR Detection System (Bio-Rad, Hercules, CA). All primer sequences used for *KRAS* mRNA and miR-217 detection are listed in supplementary Table 1 (available at *Carcinogenesis* Online). Polymerase chain reaction (PCRs) were performed at 95°C for 5 min, followed by 40 cycles of 95°C for 15 s and 60°C for 1 min. ΔCt was calculated by subtracting the Ct of *U6* or glyceraldehyde 3-phosphate dehydrogenase mRNA from the Ct of the mRNA of interest. ΔΔCt was then calculated by subtracting the ΔCt of the negative control from the ΔCt of the sample. The fold change in mRNA or miRNA was calculated according to the equation $2^{-\Delta\Delta Ct}$.

DNA and reporter vectors

DNA vectors. To construct a vector expressing miR-217 (217-vector), we amplified a 327 bp DNA fragment carrying precursor miR-217 from PANC-1 genomic DNA using the pre-miR-217 forward and reverse PCR primers; the fragment was inserted into the pcDNA 3.1 vector between the HindIII and BamHI sites.

Reporter vectors. To construct reporter vectors, the 1700 bp *KRAS* 3′-UTR containing two wild-type (WT) miR-217 recognizing sites was also amplified from PANC-1 genomic DNA using the KRAS-UTR-WT forward and reverse primers, the sequence was cloned into the pRL-TK vector between the XbaI and NotI sites. This reporter vector was called KRAS-UTR-WT.

A pRL-TK reporter vector containing the 1700 bp *KRAS* 3′-UTR with the two seed recognizing sites mutations (MUT) between the XbaI and NotI sites was constructed from KRAS-UTR-WT using PCR as follows. The KRAS-UTR-WT-forward and KRAS-UTR-MUT1-reverse primers were used to amplify the first segment A and the KRAS-UTR-MUT1-forward and KRAS-UTR-MUT2-reverse primers were used to amplify the second segment B. A and B were annealed followed by addition of the KRAS-UTR-WT-forward and KRAS-UTR-MUT2-reverse primers to amplify the annealed A + B sequence, providing the sequence containing the 1700 bp *KRAS* 3′-UTR with the two seed recognizing sites mutations (MUT). The sequence was then cloned into the pRL-TK vector between the XbaI and NotI sites. This reporter vector was called KRAS-UTR-MUT. All primers used for these constructs are listed in Supplementary Table 1 (available at *Carcinogenesis* Online).

Overexpression and inhibition of miR-217

The cells were transfected with 40 nM pre-miR-217 or 60 nM anti-miR-217 (Ambion, Austin, TX) by the reverse transfection method using the siPORT™ *NeoFX*™ transfection reagent (Ambion). Cells transfected with only the siPORT™ *NeoFX*™ transfection reagent (mock) or a scrambled sequence, either prescramble or antiscramble (Ambion), were examined in parallel as controls. Cells were then subjected to further assays or to RNA/protein extraction after 3 days. Lipofectamine 2000 (Invitrogen) was used for transfection of the 217-vector, pcDNA3.1 or reporter gene.

CCK-8 assay

The Cell Counting Kit-8 (CCK-8) (Dojindo Laboratories, Kumamoto, Japan) allows for convenient assays cell growth by utilizing a highly water-soluble tetrazolium salt. WST-8 (2-(2-methoxy-4-nitrophenyl)-3-(4-nitrophenyl)-5-(2,4-disulfophenyl)-2Htetrazolium, monosodium salt) produces a water-soluble formazan dye upon reduction in the presence of an electron mediator. Transiently transfected cells containing pre-miR-217, prescramble, 217-vector or pcDNA 3.1 were seeded in a 96-well plates (1000 cells per well). The following day, the media were replaced with 100 μl of complete medium containing 10 μl of CCK-8 solution. The plate was incubated for 1.5 h at 37°C and the absorbances at 450 nm and 630 nm were measured using a Vmax microplated spectrophotometer (Molecular Devices, Sunnyvale, CA). This procedure was repeated every day for at least 5 days for the pre-miR-217 transfection. For the 217-vector transfection, only the results from the first and fifth day were analyzed. The relative cell number is represented by the optical density (450–630 nm).

Anchorage-independent colony formation assay

Colony formation was evaluated using a soft agar colony formation assay. A total of 1.5 ml of RPMI 1640 medium containing 10% fetal bovine serum and 0.5% agar was plated on the bottom of six-well plates. The plates were stored at 4°C to allow the agar to solidify. The cells were first seeded in six-well plates for 24 h and then transfected with pre-miR-217 or anti-miR-217 for 24 h. Subsequently, the cells were trypsinized. A number of cells per well were mixed with RPMI 1640 medium containing 10% fetal bovine serum and 0.35% agar and were plated on the prepared six-well plates (three wells per condition). The plates were then transferred to 37°C. After 14 days, the colonies were scored using a microscope. Colonies were also visualized by the addition of 3-(4,5-dimethylthiazol-2-yl)-2-5-diphenyltetrazolium bromide (Sigma–Aldrich, Poole, UK) at a concentration of 500 μg/ml. Colony formation for each condition was calculated in relation to the values obtained for the scramble-treated control cells.

Xenograft tumor studies in nude mice

Male BALB/c nude mice (nu/nu; 5 weeks of age) were obtained from Vitalriver (Beijing, China). Animal handling and experimental procedures were approved by the Peking Union Medical College animal experiments Ethics committee. PANC-1 cells were injected subcutaneously into the right dorsal region of the mice to generate a primary tumor. When the tumor xenograft diameter was >7 mm, the mice were randomized into three groups of six mice per treatment group. Tumors were injected twice with 217-vector, negative pcDNA 3.1 vector or *in vivo*-jetPEI™ (201-50G; Polyplus transfection, Illkirch, France) reagent only (mock group). A total of 100 μg of 217-vector or pcDNA 3.1 was injected per mouse. *In vivo*-jetPEI™/DNA complexes were formed at an N/P ratio of 6:1. All procedures were performed according to the manufacturer's instructions. Tumor volumes and relative tumor volumes (RTVs) were calculated each week; after 5 weeks, the mice were killed and the tumors were dissected and photographed. Tumor volumes were calculated using the formula for hemi-ellipsoids: V = length (mm) × width (mm) × height (mm) × 0.5236 (23) and the RTV was determined using RTV = V_i/V_0, where V_i is the tumor volume measured weekly and V_0 is the initial tumor volume (24). Finally, the tumors were fixed in 10% formalin and embedded in paraffin. Tissue sections were obtained and stained with hematoxylin and eosin.

Prediction of miRNA targets

To investigate the miR-217 target genes and their conserved sites bound by the seed region of miR-217, the RNA22 (http://cbcsrv.watson.ibm.com/rna22.html) and PicTar (http://pitar.mdc-berlin.de/) programs were used. The sequences of the predicted mature miRNAs were confirmed by reference to miRBase (release 13.0, http://microrna.sanger.ac.uk/).

Western blot analysis

Transfected cells were lysed on ice in lysis buffer (50 mM *N*-2-hydroxyethylpiperazine-*N*′-2-ethanesulfonic acid, pH 7.5, 150 mM NaCl, 1 mM ethylenediaminetetraacetic acid, 10% glycerol and 1% Triton X-100) containing 1× complete protease inhibitor (Roche Diagnostics GmbH, Mannheim, Germany). To assess protein phosphorylation, the buffer was also supplemented with 1 mM NaVO4, 10 mM NAF and 10 mM β-glycerophosphate. Lysates were heat denatured at 100°C for 10 min before separation in 12% sodium dodecyl sulfate–polyacrylamide gels and transferred to polyvinylidene difluoride membranes (Millipore UK Ltd, Winchester, UK). Membranes were blocked with 5% bovine serum albumin in Tris-buffered saline Tween-20 buffer (10 mM Tris, pH 7.6, 150 mM NaCl and 0.1% Tween-20) and probed with primary antibody in Tris-buffered saline Tween-20 + 5% bovine serum albumin at the recommended dilutions at 4°C. Primary antibodies included KRAS (Ab-2) antibody (Santa Cruz Biotechnology Inc., Santa Cruz, CA), AKT antibody, phospho-AKT (p-AKT ser473) antibody (Cell Signaling Technology, Beverly, MA) and β-actin antibody (Santa Cruz Biotechnology Inc.). Membranes were incubated with secondary antibody (Santa Cruz Biotechnology Inc.) diluted in Tris-buffered saline Tween-20 + 5% bovine serum albumin for 1 h at room temperature. The signal was detected with the enhanced chemiluminescence system (Amersham Pharmacia Biotech, Bucks, UK) and BioMax MR-1 radiographic film (Kodak, Xiamen, China). KRAS and p-AKT protein were normalized to β-actin and total AKT, respectively.

Downloaded from https://academic.oup.com/carcin/article/31/10/1726/2477236 by guest on 24 April 2024

Immunohistochemistry analysis

Immunhistochemistry was performed according to previously described methods (25). Briefly, antigen retrieval was performed for 4 μm tissue sections in target retrieval solution (Dako, Glostrup, Denmark) by pressurized cooking at 121°C for 2.5 min in a high-pressure oven (Shunfa, Guangzhou, China). Peroxidase was then blocked by incubating the sections in 3% H_2O_2 for 30 min; protein was blocked by incubation with normal goat serum for 30 min. The sections were then incubated overnight at 4°C with KRAS polyclonal antibody BA0280 (Boster, WuHang, China) diluted 1:300 in phosphate-buffered saline, followed by biotinylated secondary antibody and peroxidase. Peroxidase-conjugated streptavidin was used with the Dako Real Detection System and diaminobenzidine (Dako, Glostrup, Denmark) according to the manufacturer's instructions. Phosphate-buffered saline was substituted for the primary antibody as a negative control. The staining intensity in the cytoplasm was assessed by experienced pathologists.

Dual-luciferase activity assay

The 1700 bp *KRAS* 3′-UTR containing two miR-217 recognizing sites (KRAS-UTR-WT) was amplified and the PCR product was subcloned into a pRL-TK vector (Promega Corporation) immediately downstream of the Renilla luciferase gene. A pRL-TK construct containing the *KRAS* 3′-UTR with the two recognizing sites mutations (KRAS-UTR-MUT) was also constructed (refer to DNA and reporter vectors). Cells were cotransfected with 500 ng of the each reporter vectors with or without pre-miR-217 precursor or anti-miR-217 for 24 to 48 h. Each sample was cotransfected with 50 ng of pGL3-control plasmid expressing Firefly luciferase to monitor the transfection efficiency (Promega Corporation). The luciferase activity assay was performed 24 to 48 h after transfection using the dual-luciferase reporter assay system (Promega Corporation). The relative luciferase activity was normalized to that of Firefly luciferase.

Statistical analysis

Statistical analysis was performed using the SPSS 13.0 software. Unless otherwise indicated, the level of significance for the difference between data sets was assessed using one-way analysis of variance. Data are expressed as the means ± SD. $P < 0.05$ was considered statistically significant.

Results

MiR-217 is downregulated in PDAC tissue and cell lines

Using locked nucleic acid *in situ* hybridization, we showed that the expression of miR-217 was significantly lower in PDAC tissues than in paired adjacent normal pancreatic tissues (Figure 1, Table I). In PDAC tissues, miR-217 was predominantly expressed in the nuclei of the ductal epithelia cells. Weak miR-217 expression was observed in five cases (5/21, 23.8%) (Figure 1G and H). No strong miR-217 staining was observed in cancer cells. In the adjacent normal pancreatic tissues, miR-217 was mainly expressed in acinar cells with variable expression levels. Weak and strong miR-217 expression levels were observed in 16 cases (16/21, 76.2%) (Figure 1C and D).

The expression of miR-217 was further assessed in a panel of seven human PDAC cell lines (PANC-1, MIAPaCa-2, AsPC-1, BxPC-3, P1, P3 and P7) and two normal pancreatic tissues (NC1 and NC2) by qPCR. The results showed that the expression of miR-217 was markedly lower in all seven PDAC cell lines than in the two normal pancreatic tissues (Figure 2A).

MiR-217 impairs tumor cell growth, anchorage-independent colony formation and in vivo xenograft tumor growth

To assess the roles of miR-217 in cell growth, CCK-8 was used to examine the growth of PANC-1 and MIAPaCa-2 cells. The rationale for using these two cell lines is that both express a relatively low level of miR-217 compared with the normal pancreatic tissue (Figure 2A). Cells that were transiently transfected with pre-miR-217 precursor (Figure 2B) or 217-vector (Supplementary Figure 1A is available at *Carcinogenesis* Online) were seeded into 96-well plates and a time course experiment was performed. Significant suppression of cell growth was observed in the pre-miR-217 and 217-vector transfection groups (Figure 2C and E, Supplementary Figure 1B is available at *Carcinogenesis* Online). Compared with mock cells, the growth of pre-miR-217-transfected cells was inhibited 30.5% (PANC-1, Figure 2D) and 24.7% (MIAPaCa-2, Figure 2F) over a period of 5 days. The growth of the 217-vector-transfected cells was inhibited 26.2% (PANC-1, Supplementary Figure 1B is available at *Carcinogenesis* Online) compared with mock cells over the same period. The prescramble or pcDNA 3.1 transfection did not affect cell growth.

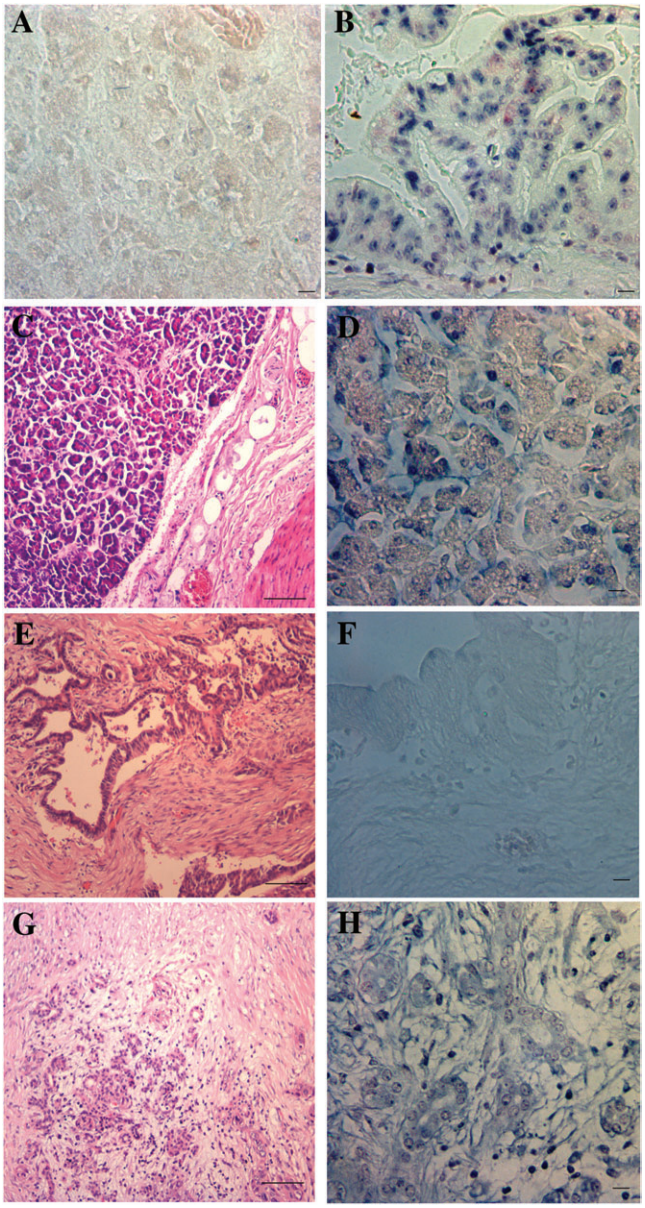

Fig. 1. Locked nucleic acid *in situ* hybridization for miR-217 in 21 PDAC and paired normal pancreas tissues. (**A** and **B**) Negative and positive control for miR-217. Horizontal bar = 10 μm. (A) Negative control for prescramble in normal pancreatic tissue. No positive staining is observed. (B) Positive control for U6 in PDAC. Note the dark nuclear staining observed in cancer cells. (**C**–**H**) Hematoxylin and eosin staining (left panels; horizontal bar = 100 μm) and miR-217 expression by *in situ* hybridization (right panels; horizontal bar = 10 μm) in normal pancreas and PDAC tissues. (C and D) Normal pancreatic tissue showing 2 + miR-217 expression. Note the dark acinar nuclear staining with cytoplasmic stippling. (E and F) PDAC tissue showing negative miR-217 expression. No staining is observed in the cancer cells. (G and H) PDAC tissue with 1 + miR-217 expression. Note the weak staining present in cancer cells.

Furthermore, miR-217 affected not only cell growth but also anchorage-independent growth (Figure 3A–D). Transfection with the pre-miR-217 precursor markedly decreased the plating efficiency of PANC-1 cells (∼65%) (Figure 3A and B) and MIAPaCa-2 cells (∼55%) (Figure 3C and D) in soft agar. The results presented in Figure 2 and Figure 3 support the hypothesis that miR-217 affects cell growth as well as anchorage-independent growth in PDAC cells.

Downloaded from https://academic.oup.com/carcin/article/31/10/1726/2477236 by guest on 24 April 2024

Table I. MiR-217 expression by *in situ* hybridization

MiR-217 expression	PDAC ($N = 21$)	Normal pancreas ($N = 21$)
Negative (0)	16	5
Weak positive (1+)	5	7
Strong positive (2+)	0	9
All positive	23.8% (5/21)*	76.2% (16/21)

*$P < 0.01$ versus normal pancreas, Fisher's exact test.

Subsequently, we evaluated the effect of the 217-vector on the growth of established tumors formed by PANC-1 cells in a subcutaneous nu/nu mouse model. For the duration of the treatment with 217-vector for 5 weeks, tumor volumes and RTVs were calculated; the mice were then killed and the tumors dissected and photographed. Tumor growth curves revealed a significant decrease in growth rates at the third, fourth and fifth week after treatment with the 217-vector, whereas no significant differences in tumor growth rates were observed between the negative pcDNA 3.1 group and the mock group (Figure 3E, Table II). Together with the inhibitory effect on cell growth demonstrated *in vitro*, these results provide strong evidence that miR-217 plays a role in the suppression of PDAC cell growth.

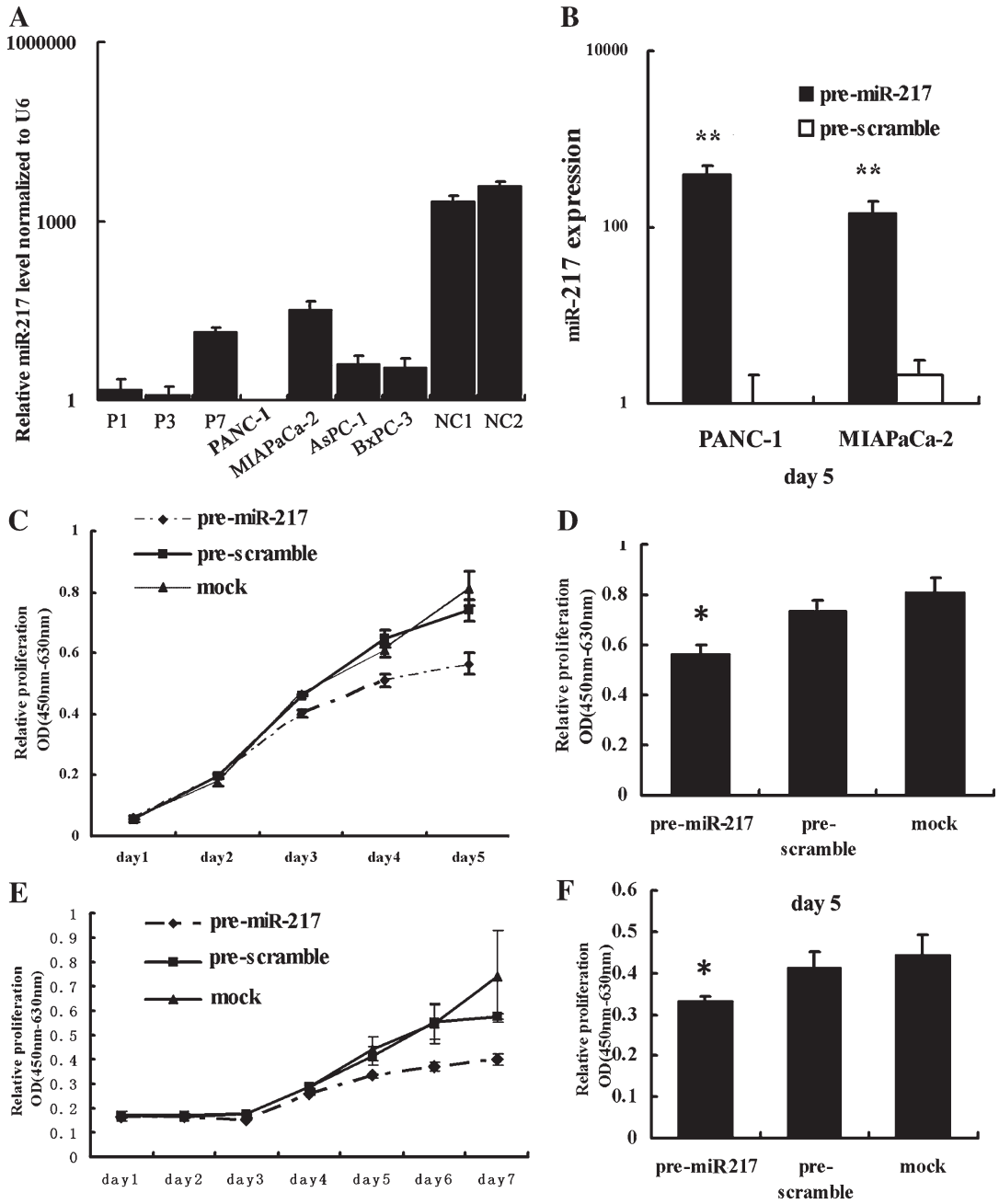

Fig. 2. Overexpression of miR-217 inhibited the growth of PANC-1 and MIAPaCa-2 cells. (**A**) MiR-217 expression in PDAC cell lines. The relative miR-217 expression in the seven PDAC cell lines was much lower than that in the two normal pancreatic tissues (NC1 and NC2) (Log_{10} scale on the *y*-axis). (**B**) Pre-miR-217 precursor transfection significantly increased the mature miR-217 level (**$P < 0.01$, Mann–Whitney test) (Log_{10} scale on the *y*-axis). The CCK-8 time course results showed that the cell growth abilities of PANC-1 (**C**) and MIAPaCa-2 (**E**) cells were inhibited after treatment with pre-miR-217. (**D**) and (**F**) show the growth results for PANC-1 and MIAPaCa-2 cells on the fifth day, respectively (*$P < 0.05$ versus prescramble or mock group).

Downloaded from https://academic.oup.com/carcin/article/31/10/1726/2477236 by guest on 24 April 2024

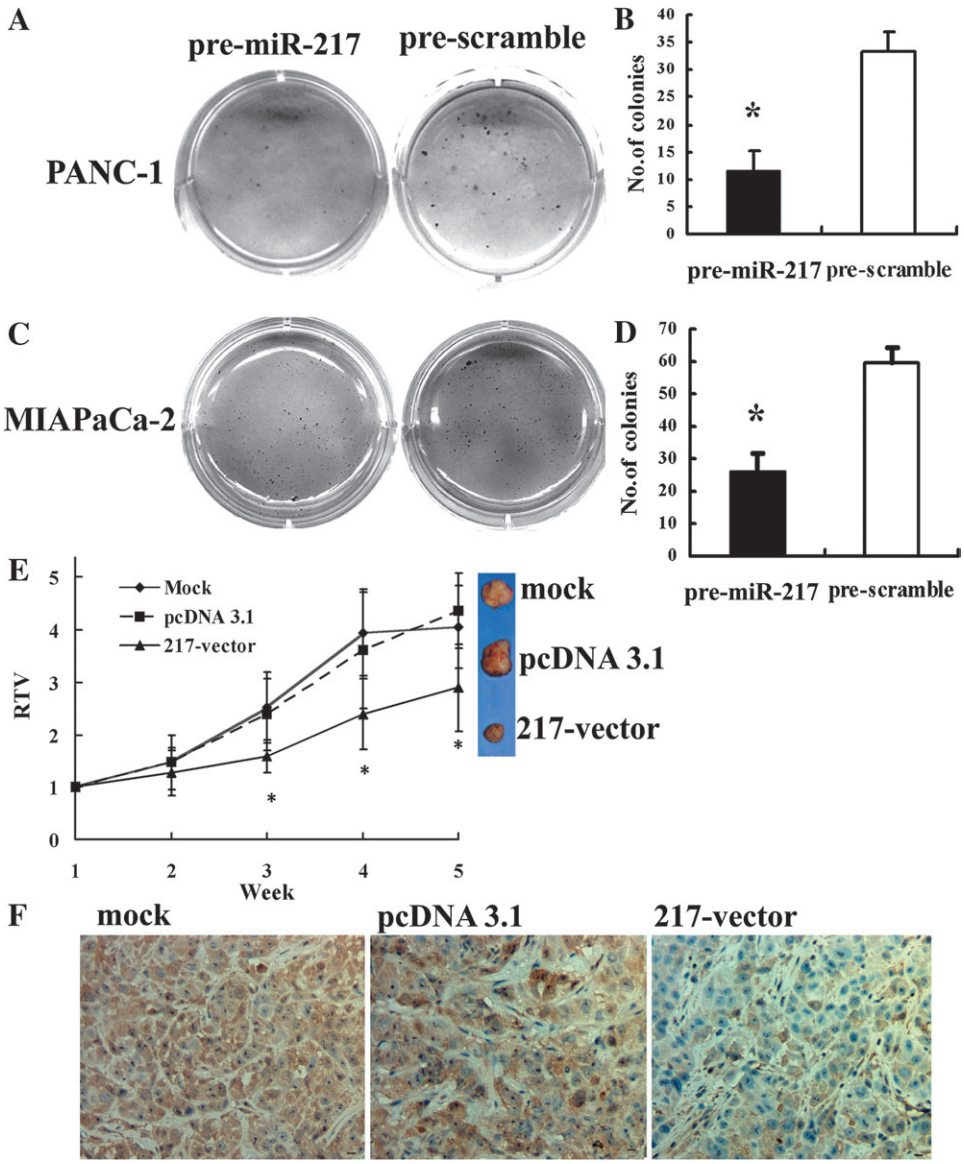

Fig. 3. Overexpression of miR-217 reduced the anchorage-independent growth ability of PDAC cells in the soft agar colony formation assay and inhibited xenograft tumor growth and KRAS expression *in vivo*. (**A**–**D**) A total of 4×10^3 cells per well were plated in 0.3% noble agar in 96-well plates for 2 weeks. The number of colonies was counted after staining with 500 μg/ml 3-(4,5-dimethylthiazol-2-yl)-2-5-diphenyltetrazolium bromide. (A and B) PANC-1 cells and (C and D) MIAPaCa-2 cells ($^*P < 0.05$, Mann–Whitney test). (**E**) PANC-1 cells were injected subcutaneously into mice and the established tumors were treated with *in vivo*-jetPEI^{TM} alone (mock), pcDNA 3.1 vector or 217-vector. The RTVs were calculated each week. The mice were then killed and the tumors were dissected and photographed. Significant differences in tumor growth between the 217-vector group and the pcDNA 3.1 group or mock group are labeled with asterisks ($^*P < 0.05$). (**F**) Overexpression of miR-217 inhibited KRAS expression in the mouse xenograft tumor. Using immunohistochemistry, the mock and pcDNA 3.1 vector groups showed relatively stronger cytoplasmic KRAS expression than did the 217-vector group. Horizontal bar = 10 μm.

Table II. Antitumor effect of the 217-vector

Groups ($n = 3$)	RTV (mm^3)			
	Second week	Third week	Fourth week	Fifth week
Mock group	1.47 ± 0.52	2.52 ± 0.68	3.94 ± 0.82	4.05 ± 0.79
pcDNA 3.1 group	1.47 ± 0.28	2.39 ± 0.69	3.61 ± 1.11	4.37 ± 0.72
217-vector group	1.27 ± 0.43	1.58 ± 0.31*	2.39 ± 0.68*	2.90 ± 0.83*

*$P < 0.05$ (versus respective mock group or pcDNA3.1 group).

In silico prediction of the miR-217 target

Using bioinformatic algorithms including RNA22 (26) and PicTar (27) for target gene prediction, *KRAS*, a key oncogene, was identified as one of the potential targets of miR-217. The predicted binding of miR-217 to the *KRAS* 3′-UTR is illustrated in Figure 4A. The sequence alignment of human miR-217 with different species of the *KRAS* 3′-UTR was found to be relatively conserved between humans and primates (Figure 4B), suggesting that KRAS is a potential direct target of miR-217.

MiR-217 regulates KRAS protein expression and AKT constitutive activation in PDAC cells

PANC-1 and MIAPaCa-2 cells were transfected with pre-miR-217, pre-scramble control, 217-vector or pcDNA 3.1 and the results showed that upregulation of miR-217 led to a dramatic reduction in *KRAS* expression at the protein level (Figure 4E and F, Supplementary Figure 1C is available at *Carcinogenesis* Online) but not at mRNA level (Figure 4H, Supplementary Figure 1D is available at *Carcinogenesis* Online). Additional data obtained by pre-miR-217 concentration gradient transfection

Downloaded from https://academic.oup.com/carcin/article/31/10/1726/2477236 by guest on 24 April 2024

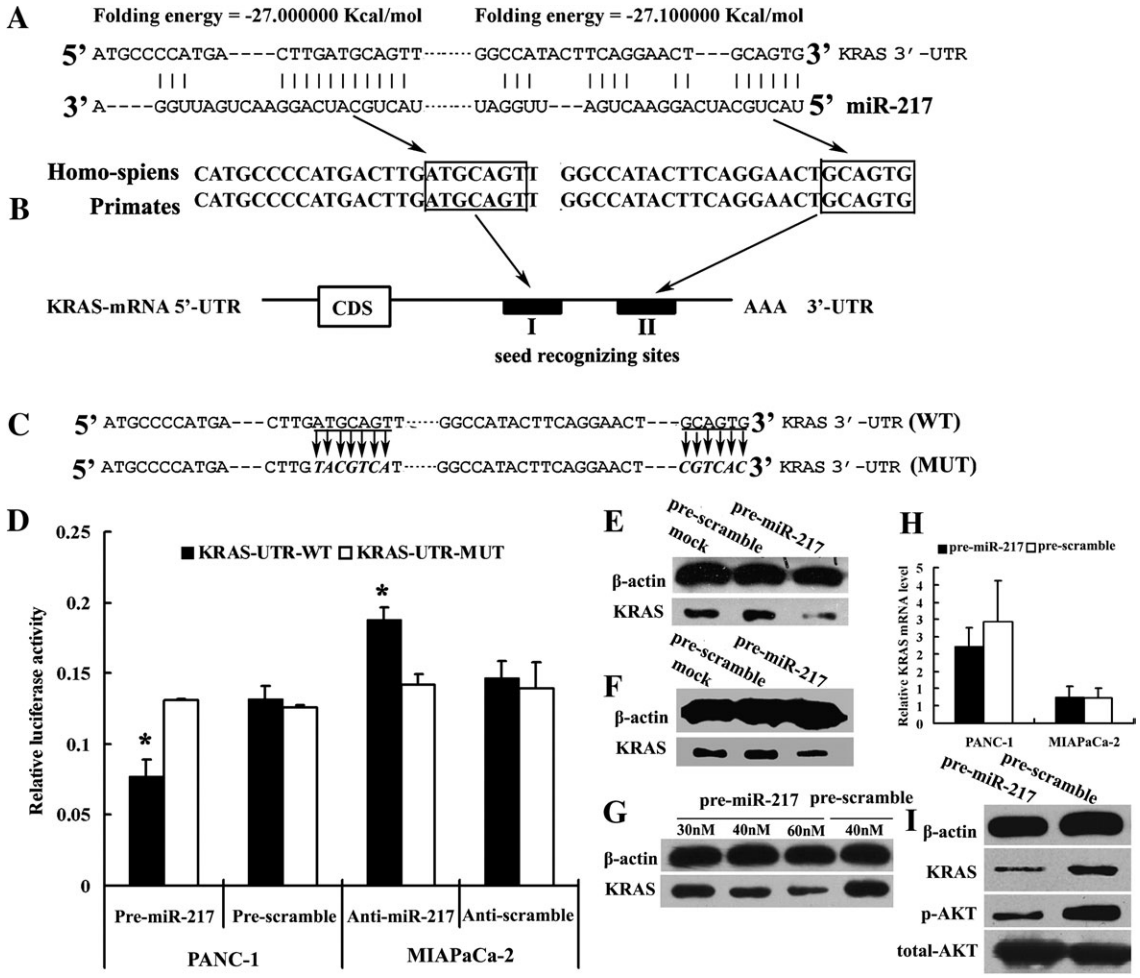

Fig. 4. KRAS is the direct target of miR-217. (**A** and **B**) *In silico* prediction of the miR-217 target. (A) Predicted binding of miR-217 to the *KRAS* 3′-UTR by RNA22. (B) Sequence alignment of human miR-217 with different species of the *KRAS* 3′-UTR by PicTar. The seed sequence of miR-217 (bracketed) matches the two seed recognizing sites of the *KRAS* 3′-UTR. (**C**) WT and two seeding recognizing sites mutated (MUT) *KRAS* 3′-UTR, with the WT seed recognizing sites (underlined) and bases substitutions MUT (italic), were subcloned into pRL-TK luciferase reporter construct are shown. (**D**) Overexpression of miR-217 inhibited WT but not mutant *KRAS* 3′-UTR reporter activity in PANC-1 cells. MiR-217 inhibition increased WT but not mutant *KRAS* 3′-UTR reporter activity in MIAPaCa-2 cells ($^*P < 0.05$). (**E–I**) MiR-217 overexpression decreased the levels of KRAS and phospho-AKT protein. Western blot and qPCR were used to detect the protein and mRNA levels, respectively. Overexpression of miR-217 significantly inhibited the KRAS protein expression level in both PANC-1 (E) and MIAPaCa-2 cells (F), but no significant change was detected at the *KRAS* mRNA level (H). When PANC-1 cells were treated with 30 nM, 40 nM or 60 nM pre-miR-217, KRAS protein was downregulated. This downregulation correlated with the concentration of miR-217 (G). Phospho-AKT protein level in PANC-1 cells decreased following transfection with pre-miR-217 (I).

in PANC-1 cells showed that downregulation of KRAS protein depended on the concentration of miR-217 (Figure 4G), suggesting the potential posttranscriptional regulation of *KRAS* by miR-217.

Previous reports have shown that *KRAS* gene activation will trigger the RAS/PI3K/AKT signaling pathway, which regulates cell survival, size and proliferation (28–30). Mounting evidence indicates that this pathway plays an important role in PDAC (1). To detect the constitutive activation level of AKT following upregulation of miR-217, we assessed p-AKT expression in PANC-1 cells by western blotting. Our data demonstrated that upregulation of miR-217 via pre-miR-217 could decrease both KRAS protein expression and the level of constitutive AKT activation (Figure 4I).

Next, we analyzed KRAS protein expression in nude mice xenograft tumor tissues from each group by immunhistochemistry. The 217-vector group demonstrated the lowest level of KRAS protein expression among the three groups (Figure 3F). This result indicates that miR-217 can inhibit KRAS expression *in vivo*.

KRAS is a direct target of miR-217

To further confirm that KRAS is a direct target of miR-217, a 1700 bp segment of the 3′-UTR of *KRAS*, with or without seed sequence recognizing sites mutations (Figure 4C), was subcloned downstream of the Renilla luciferase reporter. The constructs were then cotransfected with pre-miR-217 precursor or anti-miR-217 or with the pre-scramble or antiscramble controls for the luciferase activity assays. The relative luciferase activity of the WT construct of the *KRAS* 3′-UTR in PANC-1 cells was significantly reduced in the presence of pre-miR-217 ($P < 0.05$); the relative luciferase activity of the WT construct of the KRAS 3′-UTR in MIAPaCa-2 cells was significantly increased in the presence of anti-miR-217 ($P < 0.05$). However, this effect was not observed in either cell line carrying the MUT construct of the *KRAS* 3′-UTR, highlighting the direct and specific interaction of miR-217 with the *KRAS* 3′-UTR (Figure 4D).

Inhibition of miR-217 upregulates KRAS protein expression and increases anchorage-independent colony formation ability in PDAC cells

Previous results have shown that miR-217 can directly inhibit the expression of KRAS protein, PDAC cell and xenograft tumor growth and anchorage-independent colony formation. To further validate whether the inhibition of miR-217 can increase KRAS levels and facilitate PDAC progression, we assessed KRAS protein expression

Downloaded from https://academic.oup.com/carcin/article/31/10/1726/2477236 by guest on 24 April 2024

and the growth of MIAPaCa-2 cells by western blot and the anchorage-independent colony formation assay, respectively, after inhibiting endogenous miR-217 expression. We found that transfection with the anti-miR-217 inhibitor significantly upregulated KRAS at the protein level (Supplementary Figure 2A and C is available at *Carcinogenesis* Online) but not at the mRNA level (Supplementary Figure 2B is available at *Carcinogenesis* Online) and markedly increased the plating efficiency of MIAPaCa-2 cells (~67%) in soft agar, when compared with the scramble control (Supplementary Figure 2D and E is available at *Carcinogenesis* Online). These findings further support the results of the overexpression experiment.

Relationship between the expression of miR-217 and KRAS in PDAC cell lines

To further confirm the correlation between KRAS protein and miR-217 expression levels, we assessed the expression levels of miR-217 and *KRAS* mRNA and protein in the seven PDAC cell lines by qPCR and western bloting, respectively (Supplementary Figure 3 is available at *Carcinogenesis* Online). As shown in Supplementary Figure 3C (available at *Carcinogenesis* Online), a negative correlation between miR-217 and KRAS protein expression was observed in all PDAC cell lines ($r = -0.821$, $P = 0.023$; Spearman's correlation). However, this relationship was not observed between miR-217 and *KRAS* mRNA expression ($r = -0.741$, $P > 0.05$; Spearman's correlation; Supplementary Figure 3E is available at *Carcinogenesis* Online).

Discussion

The frequent aberrant expression of miRNAs implies that they have a tumor suppressor or oncogene function. Under certain circumstances, one miRNA may be expressed in different cellular locations. For example, miR-21 is predominantly expressed in the cytoplasm of luminal cells in breast cancer (31), whereas miR-21 staining is observed in the nuclei of ductal epithelial cells in pancreatitis and is predominantly expressed in the nuclei of tumor cells with some cytoplasmic stippling in pancreatic cancer (21). This information prompted us to examine the expression, cellular location and roles of miR-217 in PDAC development.

In agreement with previous miRNA expression profiles and qPCR results (14,32), the present study demonstrated that miR-217 was significantly downregulated in 21 PDAC patient tissue samples and 7 PDAC cell lines. Our locked nucleic acid *in situ* hybridization results further showed that miR-217 was mainly expressed in the nuclei of tumor ductal epithelial cells and normal pancreatic acinar cells. There is no clear evidence demonstrating the specific function(s) of either cytoplasmic or nuclear miRNA. However, there is a evidence that small RNAs, including miRNAs, play important nuclear roles and that some miRNAs may revisit the nucleus after being exported to the cytoplasm (33). We speculate that the cellular location of miRNAs may influence their functional significance.

Based on the association between abnormal miRNA expression and disease, two major miRNA-based therapeutic strategies are to restore the expression of reduced miRNA expression in disease and, conversely, to abrogate overexpressed miRNA (34). In this study, we found that overexpression of miR-217 significantly reduced PDAC cell growth and anchorage-independent colony formation. Importantly, *in vivo* xenograft tumor growth curves revealed a significant decrease in tumor growth rates following treatment with the miR-217 expression vector. These results indicate that miR-217 can reverse the malignant behavior of PDAC cells and may have a promising future for the treatment of PDAC.

Furthermore, we showed that miR-217 is a tumor suppressor and exerts its function by specifically targeting the *KRAS* oncogene. Additionally, the expression of p-AKT, a downstream molecule in KRAS signaling, was affected by miR-217 overexpression. These observations further indicate that miR-217 affects the KRAS signaling pathway.

KRAS is a crucial molecule in the development and progression of pancreatic cancer (35). Mutation of the *KRAS* oncogene is the most frequent genetic alteration associated with pancreatic cancer as it has been identified in up to 90% of all PDAC cases (36). Activating mutations of RAS-family oncogenes produce a significant array of cellular effects, including induction of proliferation, survival and invasion through the stimulation of several downstream effector pathways (37), such as the PI3K/AKT pathway, the RAF/ERK pathway, nuclear factor-kappaB, among others (1,38).

Although mutation is one cause of RAS activation, the expression level and activity of the RAS oncogene can be regulated at different stages, e.g. gene transcriptional activity, posttranslational cellular localization, etc (39). Recently, miRNAs were shown to be involved in the posttranscriptional regulation of RAS. For example, let-7 miRNA can target RAS, which suppresses the development of different cancers (10,40,41). In the present study, an important molecular association between miR-217 and KRAS was demonstrated. First, KRAS protein expression in PANC-1, MIAPaCa-2 cells and in PANC-1 nude mouse xenograft tumors was significantly downregulated following upregulation of miR-217 via pre-miR-217 precursor and 217-vector, respectively, whereas the anti-miR-217 inhibitor upregulated KRAS protein expression in MIAPaCa-2 cells. Second, loss-of-function evaluation of KRAS through the upregulation of miR-217 expression suppressed tumor cell growth, anchorage-independent colony formation and *in vivo* xenograft tumor growth. Concurrently, gain-of-function analysis of KRAS via the downregulation of miR-217 expression facilitated anchorage-independent colony formation. Third, the negative correlation between miR-217 and KRAS protein expression in the PDAC cell lines further indicated that downregulation of miR-217, which results in upregulation of KRAS, is a potentially important feature in PDAC development. Fourth, the downregulation of KRAS expression by miR-217 inhibited the constitutive phosphorylation of AKT, a downstream molecule in KRAS signaling. Finally, our dual-luciferase reporter gene results also provided evidence that KRAS is a direct target of miR-217. Taken together, the present findings demonstrate that miR-217 can regulate KRAS expression and function as a tumor suppressor in PDAC development.

In summary, this study confirms that miR-217 is frequently downregulated in PDAC and is a potential tumor-suppressing miRNA in PDAC development. The regulation of KRAS and KRAS signaling by miR-217 might play a role in the regulation of malignant PDAC behavior. Therefore, miR-217 may serve as a useful therapeutic agent for miRNA-based PDAC therapy.

Supplementary material

Supplemental Figures 1–3 and Table 1 can be found at http://carcin.oxfordjournals.org/.

Funding

National Natural Science Foundation of China (30270599, 30471970); National Science and Technology Support Project of China (115 program) (2006BAI02A14).

Acknowledgement

Conflict of Interest Statement: None declared.

References

1. Hezel,A.F. *et al*. (2006) Genetics and biology of pancreatic ductal adenocarcinoma. *Genes Dev.*, **20**, 1218–1249.
2. Bardeesy,N. *et al*. (2002) Pancreatic cancer biology and genetics. *Nat. Rev. Cancer*, **2**, 897–909.
3. Hruban,R.H. *et al*. (2006) Pancreatic cancer in mice and man: the Penn Workshop 2004. *Cancer Res.*, **66**, 14–17.

Downloaded from https://academic.oup.com/carcin/article/31/10/1726/2477236 by guest on 24 April 2024

4. Schneider,G. *et al*. (2005) Pancreatic cancer: basic and clinical aspects. *Gastroenterology*, **128**, 1606–1625.
5. Bartel,D.P. (2004) MicroRNAs: genomics, biogenesis, mechanism, and function. *Cell*, **116**, 281–297.
6. Lee,E.J. *et al*. (2007) Expression profiling identifies microRNA signature in pancreatic cancer. *Int. J. Cancer*, **120**, 1046–1054.
7. Lu,J. *et al*. (2005) MicroRNA expression profiles classify human cancers. *Nature*, **435**, 834–838.
8. Volinia,S. *et al*. (2006) A microRNA expression signature of human solid tumors defines cancer gene targets. *Proc. Natl Acad. Sci. USA*, **103**, 2257–2261.
9. Esquela-Kerscher,A. *et al*. (2006) Oncomirs—microRNAs with a role in cancer. *Nat. Rev. Cancer*, **6**, 259–269.
10. Akao,Y. *et al*. (2006) let-7 microRNA functions as a potential growth suppressor in human colon cancer cells. *Biol. Pharm. Bull.*, **29**, 903–906.
11. Cimmino,A. *et al*. (2005) miR-15 and miR-16 induce apoptosis by targeting BCL2. *Proc. Natl Acad. Sci. USA*, **102**, 13944–13949.
12. Takagi,T. *et al*. (2009) Decreased expression of microRNA-143 and -145 in human gastric cancers. *Oncology*, **77**, 12–21.
13. Griffiths-Jones,S. *et al*. (2008) miRBase: tools for microRNA genomics. *Nucleic Acids Res.*, **36**, D154–D158.
14. Szafranska,A.E. *et al*. (2007) MicroRNA expression alterations are linked to tumorigenesis and non-neoplastic processes in pancreatic ductal adenocarcinoma. *Oncogene*, **26**, 4442–4452.
15. Menghini,R. *et al*. (2009) MicroRNA 217 modulates endothelial cell senescence via silent information regulator 1. *Circulation*, **120**, 1524–1532.
16. Hida,Y. *et al*. (2007) Strong expression of a longevity-related protein, SIRT1, in Bowen's disease. *Arch. Dermatol. Res.*, **299**, 103–106.
17. Huffman,D.M. *et al*. (2007) SIRT1 is significantly elevated in mouse and human prostate cancer. *Cancer Res.*, **67**, 6612–6618.
18. Yeung,F. *et al*. (2004) Modulation of NF-kappaB-dependent transcription and cell survival by the SIRT1 deacetylase. *EMBO J.*, **23**, 2369–2380.
19. Kato,M. *et al*. (2009) TGF-beta activates Akt kinase through a microRNA-dependent amplifying circuit targeting PTEN. *Nat. Cell Biol.*, **11**, 881–889.
20. Chen,J. *et al*. (1990) Two new human exocrine pancreatic adenocarcinoma cell lines *in vitro* and *in vivo*. *Chin. Med. J. (Engl.)*, **103**, 369–375.
21. Dillhoff,M. *et al*. (2008) MicroRNA-21 is overexpressed in pancreatic cancer and a potential predictor of survival. *J. Gastrointest. Surg.*, **12**, 2171–2176.
22. Chen,C. *et al*. (2005) Real-time quantification of microRNAs by stem-loop RT-PCR. *Nucleic Acids Res.*, **33**, e179.
23. Maeda,H. *et al*. (2000) Rapid detection of candidate metastatic foci in the orthotopic inoculation model of androgen-sensitive prostate cancer cells introduced with green fluorescent protein. *Prostate*, **45**, 335–340.
24. Emmrich,S. *et al*. (2009) Antisense gapmers selectively suppress individual oncogenic p73 splice isoforms and inhibit tumor growth *in vivo*. *Mol. Cancer*, **8**, 61–73.
25. Lai,K.W. *et al*. (2010) MicroRNA-130b regulates the tumour suppressor RUNX3 in gastric cancer. *Eur. J. Cancer*, **46**, 1456–1463.
26. Miranda,K.C. *et al*. (2006) A pattern-based method for the identification of microRNA binding sites and their corresponding heteroduplexes. *Cell*, **126**, 1203–1217.
27. Lall,S. *et al*. (2006) A genome-wide map of conserved microRNA targets in *C. elegans*. *Curr. Biol.*, **16**, 460–471.
28. Cantley,L.C. (2002) The phosphoinositide 3-kinase pathway. *Science*, **296**, 1655–1657.
29. Rodriguez-Viciana,P. *et al*. (1996) Activation of phosphoinositide 3-kinase by interaction with Ras and by point mutation. *EMBO J.*, **15**, 2442–2451.
30. Vivanco,I. *et al*. (2002) The phosphatidylinositol 3-Kinase AKT pathway in human cancer. *Nat. Rev. Cancer*, **2**, 489–501.
31. Qi,L. *et al*. (2009) Expression of miR-21 and its targets (PTEN, PDCD4, TM1) in flat epithelial atypia of the breast in relation to ductal carcinoma in situ and invasive carcinoma. *BMC Cancer*, **9**, 163.
32. Szafranska,A.E. *et al*. (2008) Analysis of microRNAs in pancreatic fine-needle aspirates can classify benign and malignant tissues. *Clin. Chem.*, **54**, 1716–1724.
33. Politz,J.C. *et al*. (2009) MicroRNAs with a nucleolar location. *RNA*, **15**, 1705–1715.
34. Tsai,L.M. *et al*. (2010) MicroRNAs in common diseases and potential therapeutic applications. *Clin. Exp. Pharmacol. Physiol.*, **37**, 102–107.
35. Furukawa,T. (2009) Molecular pathology of pancreatic cancer: implications for molecular targeting therapy. *Clin. Gastroenterol. Hepatol.*, **7**, S35–S39.
36. Almoguera,C. *et al*. (1988) Most human carcinomas of the exocrine pancreas contain mutant c-K-ras genes. *Cell*, **53**, 549–554.
37. Shields,J.M. *et al*. (2000) Understanding Ras: 'it ain't over 'til it's over'. *Trends Cell. Biol.*, **10**, 147–154.
38. Downward,J. (2003) Targeting RAS signalling pathways in cancer therapy. *Nat. Rev. Cancer*, **3**, 11–22.
39. Tsang,W.P. *et al*. (2009) The miR-18a* microRNA functions as a potential tumor suppressor by targeting on K-Ras. *Carcinogenesis*, **30**, 953–959.
40. Johnson,S.M. *et al*. (2005) RAS is regulated by the let-7 microRNA family. *Cell*, **120**, 635–647.
41. Kumar,M.S. *et al*. (2008) Suppression of non-small cell lung tumor development by the let-7 microRNA family. *Proc. Natl Acad. Sci. USA*, **105**, 3903–3908.

Received June 2, 2010; revised July 21, 2010; accepted July 27, 2010

Downloaded from https://academic.oup.com/carcin/article/31/10/1726/2477236 by guest on 24 April 2024